A Comparison of Kernel-Driven BRDF Parameters Between AHI and VIIRS for Surface Reflectance Characterization

Masayuki Matsuoka[1]*, Hiroki Yoshioka[2], Kazuhito Ichii[3]

[1]*Mie University, 1577 Kurima-machiya, Tsu, Mie, Japan. matsuoka@info.mie-u.ac.jp*
[2]*Aichi Prefectural University, Nagakute, Aichi, Japan.*
[3]*Chiba University, Chiba, Japan.*

Abstract: We compared the parameters of the kernel-driven Bidirectional Reflectance Distribution Function (BRDF) model between the geostationary Advanced Himawari Imager (AHI) and the polar-orbiting Visible Infrared Imaging Radiometer Suite (VIIRS). The AHI-derived parameters were terrain-dependent and could not accurately reproduce hotspot reflectance near local noon. Moreover, reflectance estimated for AHI using VIIRS-derived parameters showed poor agreement with observations. These discrepancies highlight the need for further refinement of the BRDF model.

Keywords: Bidirectional reflectance, GEO-LEO comparison

1. Introduction

Data fusion of geostationary Earth orbit (GEO) and low Earth orbit (LEO) satellites has become an active research topic in remote sensing. The complementary strengths of high-temporal-resolution GEO data and high-spatial-resolution LEO data provides valuable information for understanding environmental systems on Earth.

The Bidirectional Reflectance Distribution Function (BRDF) model simulates sensor-observed reflectance based on the geometry of the satellite, the Sun, and the Earth's surface. The kernel-driven BRDF model is commonly used in sensors with wide observation swaths, such as the Moderate Resolution Imaging Spectroradiometer (MODIS) and the Visible Infrared Imaging Radiometer Suite (VIIRS). This model is also used to estimate land surface albedo by accumulating reflectance values in all directions using estimated kernel parameters.

Although there are differences in the spectral response function, the BRDF parameters for GEO and LEO would be similar if the model were perfect. Additionally, comparing GEO-LEO BRDFs is useful for improving BRDF models. The objective of this study is to compare the parameters in the kernel-driven BRDF model for AHI and VIIRS.

2. Methodology

For the AHI data, we used the Himawari Japan Area data provided by the Japan Meteorological Agency (JMA) through the National Institute of Information and Communications Technology (NICT) Science Cloud (NICT 2025). We analyzed bands 3, 4, and 5, corresponding to the red, near infrared, and shortwave infrared regions, respectively. After reducing geometric errors using ground

control points (Matsuoka 2016), the data was orthorectified onto a latitude-longitude projection (Matsuoka 2023). The spatial resolutions of bands 3, 4, and 5 were 0.005°, 0.01°, and 0.02°, corresponding to the original ground resolutions of 500, 1000, and 2000 m, respectively. The reflectance values were atmospherically corrected by 6S code (Vermote 1997). The clouds were then detected by comparing the red reflectance to the cloud-free composite image. We evaluated four kernel combinations: two volume kernels, Ross-Thick (RTK) and Ross-Thin (RTN), and two geometric kernels, Li-Sparse-Reciprocal (LSR) and Li-Dense (LDN). Parameters were estimated using ordinary multiple regression.

For VIIRS data, we used the product "VIIRS/NPP BRDF/Albedo Model Parameters Daily L3 Global 500m SIN Grid V002 (VNP43IA1)", downloaded from NASA Earthdata Search. The bands I1, I2, and I3 were used to match the AHI bands 3, 4, and 5, respectively. The data were reprojected to the same map projection as the AHI data. The spatial resolution was 0.005° for all bands, which reflects the original resolution of the sensor.

The AHI data consisted of observations acquired on October 13, 2024, and April 30, 2025, during the period from 8:00 to 16:00 JST. The Japan Area data is acquired every 2.5 minutes, resulting in 193 observation scenes per day. The same dates were used for the VNP43IA1 product. As VIIRS typically provides one daytime observation per day, 16 consecutive days of data were employed to estimate the BRDF parameters centered on day nine (Schaaf 2017).

3. Results and discussion

Table 1 shows the root mean square (RMS) residuals of regression for each kernel combination. The best combination of the kernel changes with the season. Although these values represent scene averages, the optimal kernel combination may vary by location, even on the same observation day. For the following results, we selected the Ross-Thick (RTK) and Li-Sparse-Reciprocal (LSR) kernels to reflect the kernel combinations used in the VIIRS algorithm.

Table 1: RMS residuals by kernel combination.

		Kernel combination			
Date	Band	RTK_LDN	RTK_LSR	RTN_LDN	RTN_LSR
Oct. 13	3	0.0048	0.0050	0.0050	0.0051
	4	0.0162	0.0172	0.0186	0.0180
	5	0.0080	0.0094	0.0087	0.0094
Apr. 30	3	0.0039	0.0040	0.0045	0.0044
	4	0.0066	0.0066	0.0082	0.0077
	5	0.0033	0.0032	0.0040	0.0037

Figure 1 illustrates the geographic distribution of the estimated kernel parameters on April 30, 2025, in central Japan. The f_{iso} parameter exhibited spatial similarity due to its assumption of normalized, angular-independent reflectance. The VIIRS f_{iso} value distribution was approximately 0.05 higher than the AHI f_{iso} value. The three parameters of AHI were clearly dependent on topography.

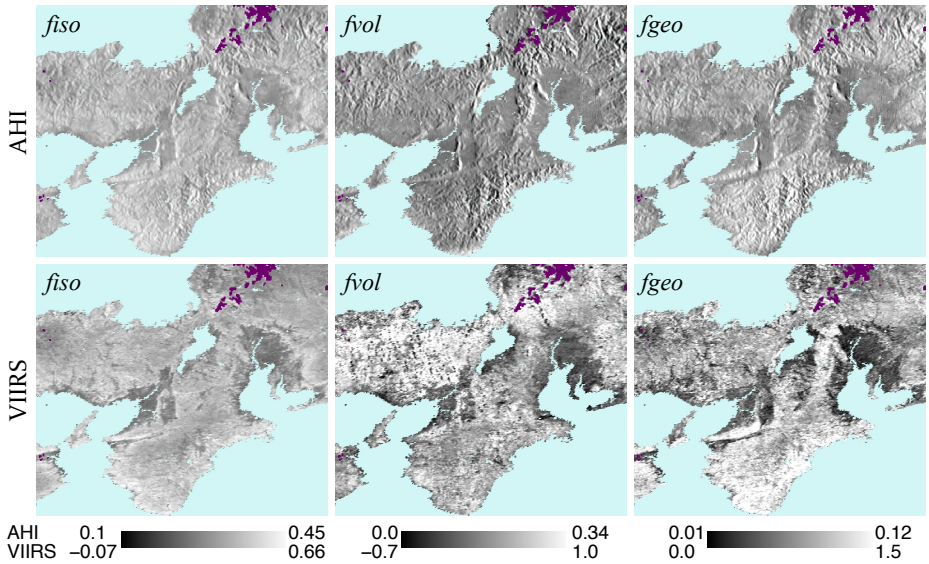

Figure 1: Estimated kernel parameters for April 30, 2025. Purple shows the cloud mask.

Figure 2 shows the polar coordinate plot of the observation geometry for AHI and VIIRS. AHI is capable of capturing variations in shadow patterns caused by the diurnal movement of the sun. VIIRS acquires data at an almost constant local observation time, which limits its ability to capture shadow variations caused by terrain or solar position.

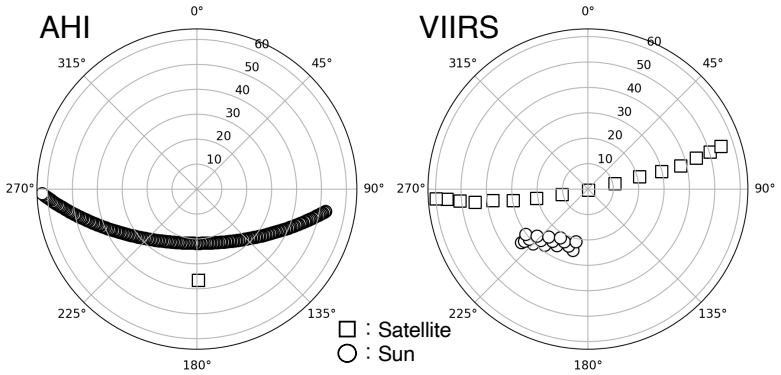

Figure 2: Observation geometry of AHI and VIIRS.

The left three columns of Figure 3 present a comparison between observed and estimated reflectance. The black dots indicate the observed reflectance, while the black and gray lines denote the reflectance estimated using the AHI and VIIRS parameters, respectively. The rightmost column of Figure 3 illustrates the values of the four kernel functions, with the RTK and LSR kernels adopted in this analysis. As shown in the top panels, the sharp peak (hotspot) reflectance around noon on October 13 was not reproduced because neither kernel showed a sharp change. It suggests that the BRDF model should be expanded to include a hotspot (Yang, 2025). The estimated AHI values using VIIRS parameters did not match the actual AHI reflectance. It is a challenging task to improve BRDF models that match both.

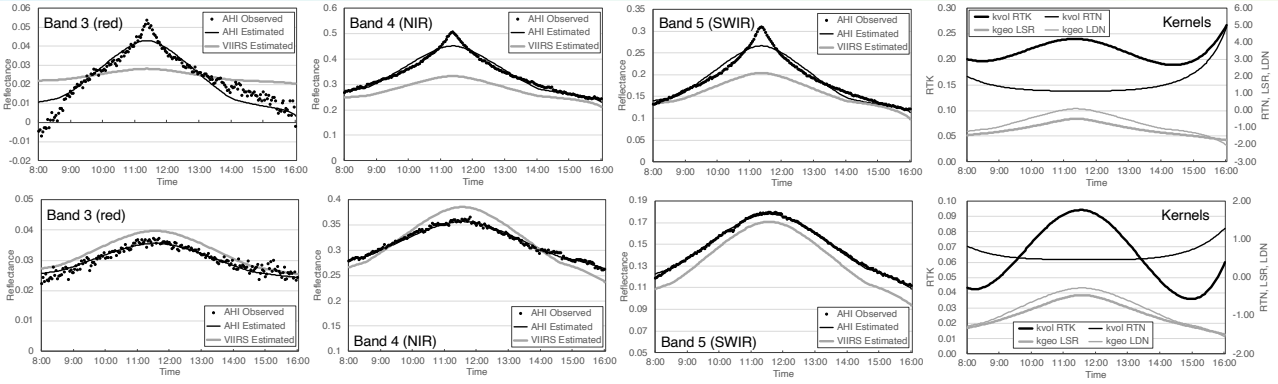

Figure 3: Time series of the observed and estimated reflectance values on October 13, 2024 (top) and April 30, 2025 (bottom). The rightmost panels show the four kernel values.

4. Conclusion

Further refinement is required to enable effective GEO–LEO data fusion because kernel-driven models provide realistic methodology for representing the bidirectional reflectance.

Acknowledgment

This work was supported by JSPS KAKENHI Grant Numbers JP21K05669, JP22H05004, and JP20K20487.

References

Matsuoka, M., R. Honda, A. Nonomura, H. Moriya, S. Akatsuka, H. Yoshioka and M. Takagi, 2016. A Method to Improve Geometric Accuracy of Himawari-8/AHI "Japan Area" Data, *Journal of the Japan society of photogrammetry and remote sensing*, 54(6), pp. 280-289. https://doi.org/10.4287/jsprs.54.280

Matsuoka, M. and H. Yoshioka, 2023. Orthorectification of Data from the AHI Aboard the Himawari-8 Geostationary Satellite, *Remote Sensing*, 15(9), 2403. https://doi.org/10.3390/rs15 0924 03

NICT, 2025. NICT Science Cloud. https://sc-web.nict.go.jp/sciencecloud (accessed on 18/09/2025).

Schaaf, C.B., 2017. VIIRS BRDF, Albedo, and NBAR Product Algorithm Theoretical Basis Document (ATBD), https://lpdaac.usgs.gov/documents/194/VNP43_ATBD_V1.pdf (accessed on 21/09/2025)

Vermote, E.F., D. Tanré, J.L. Deuzé, M. Herman, and J.-J. Morcrette, 1997. Second Simulation of the Satellite Signal in the Solar Spectrum, 6S: An Overview, *IEEE Transactions on Geoscience and Remote Sensing*, 35(3), pp. 675-686. https://doi.org/10.1109/36.581987 also https://salsa. umd.edu/ 6spage.html (accessed on 18/09/2025)

Yang, W., Z. Qiao, W. Li, X. Ma, K. Ichii, 2025. An Enhanced RPV Model to Better Capture Hotspot Signatures in Vegetation Canopy Reflectance Observed by the Geostationary Meteorological Satellite Himawari-8, Science of Remote Sensing, 11, 100222. https://doi.org/10.1016/j.srs.2025.100222